Journal of the American Ceramic Society

# Stability of BiVO3 perovskite: theoretical and experimental investigation

| | |
|---|---|
| Journal: | *Journal of the American Ceramic Society* |
| Manuscript ID: | JACERS-31935 |
| Manuscript Type: | Article |
| Date Submitted by the Author: | 22-Aug-2012 |
| Complete List of Authors: | Dragomir, Mirela; University of Nova Gorica, Materials Research Laboratory<br>Praveen, Chandramathy; University of Nova Gorica, Materials Research Laboratory<br>Valant, Matjaz; University of Nova Gorica, Materials Research Laboratory; Center of Excellence for Biosensors, Instrumentation and Process Control, |
| Keywords: | perovskites, reduction, X-ray methods |
| | |

# Stability of $BiVO_3$ perovskite: theoretical and experimental investigation

**Mirela Dragomir[*a], Chandramathy Surendran Praveen [a] and MatjazValant[a,b]**

[a]*Materials Research Laboratory, University of Nova Gorica, SI-5270, Ajdovščina, Slovenia.*

[b]*Center of Excellence for Biosensors, Instrumentation and Process Control, SI-5250, Solkan, Slovenia*



**The structural and dynamical stability of the $BiVO_3$ perovskite has been investigated by ab-initio calculations and experimental studies. Our calculated ground-state structure for $BiVO_3$ has Pnma symmetry with ferromagnetic spin ordering. The computational modelling suggests that the compound is dynamically stable at its ground state. The experimental study showed that the synthesis at elevated temperatures cannot be performed due to strong orbital interaction of the $Bi^{3+}$ and $V^{3+}$ atoms with oxygen that facilitates the electron transfer from V to Bi and destabilize the structure. The process yields metallic Bi and oxidized Bi-vanadate phases. Therefore, the conditions for the synthesis of $BiVO_3$ are limited to low temperatures, for which the activation energy for the reduction-oxidation process is not exceed.**

## I. Introduction

Over the last decades, bismuth-based compounds have been extensively studied because of their extraordinary properties originating from the electronic and/or steric influences of the $6s^2$ lone pair of $Bi^{3+}$. Another important reason for such interest in these materials is the relatively low toxicity

*Author to whom correspondence should be addressed: e-mail: mirela.dragomir@ung.si

compared to other related compounds containing heavy metals with similar electronic structure (e.g. Hg, Cd, Sn, Tl or Pb). This makes Bi(III) compounds promising candidates for a variety of applications where substitution of e.g. Pb is required in order to satisfy environmental requirements. The broad spectrum of applications of Bi compounds ranges from pigments, cosmetic products, biocompatible additives in medicine, superconductors, sensors, ion conducting solid electrolytes, luminescent materials, catalysts, to thermoelectric or ferroelectric materials.[1-5] In the last years, the interest in the Bi-compounds, especially perovskites, have further escalated due to their potential as lead-free piezoelectrics ($BiAlO_3$, $BiScO_3$, $BiFeO_3$, $BiCoO_3$, $BiGaO_3$ and modified versions of these compounds),[6-10] photocatalysts ($BiFeO_3$, Ga-doped $BiFeO_3$),[11-13] and multiferroics ($BiFeO_3$, $BiMnO_3$, $BiCoO_3$, $BiCrO_3$).[14-20] As a consequence, these compounds have been thoroughly investigated and significant amount of knowledge has been accumulated. Also for other Bi-perovskites, interesting properties have been discovered such as negative thermal expansion and giant magneto-optical Kerr effect in $BiNiO_3$.[21,22]

In addition to the mentioned compounds, there is a group of simple Bi-perovskites that has not been synthesized yet. There is no information available in the literature about the existence of $BiVO_3$, $BiTiO_3$ or $BiCuO_3$.[23] It would be wrong to assume that the lack of the literature reports on these compounds indicates that they are not stable. For instance, $BiAlO_3$ has not been synthesized for long time but only after an ab-initio computational study predicted its thermodynamic stability and promising piezoelectric properties, enough experimental efforts have been invested to synthesize it.[6,24]

The present study focuses on $BiVO_3$ perovskite, for which promising photocatalytic and/or multiferroic properties can be expected by analogy to similar $BiFeO_3$ and $BiMnO_3$ systems. The special role of $Bi^{3+}$ in the photocatalysis comes from its Bi $6s^2$ lone electron pair that hybridizes with the O *2p* orbitals, which results in an increase in the valence band level.[25] This is why the Bi-

based oxide semiconductors exhibit untypically low band gaps (e.g. the band gaps of $Bi_2Ti_2O_7$,[26] $BiFeO_3$[11] or $BiVO_4$[27] were found to be 2.8, 2.5, and 2.4 eV, respectively). In $BiVO_3$, both Bi and V are in 3+ oxidation state, so the partially filled *d* orbitals of $V^{3+}$are available to induce the ferromagnetism, while the Bi *6s*-O *2p* hybridization could be responsible for distortion of the Bi coordination environment resulting in the ferroelectricity. The coupling of the ferroelectricity with the ferromagnetism would further give rise to multiferroic properties, which are of high fundamental importance for material scientists as well as of high applied value for modern technologies.

Empirical approaches that are used to estimate stability of perovskites predict that $BiVO_3$ should be stable. The Goldschmidt tolerance factor (t)[28] for $BiVO_3$ is 0.892 (for ionic radii reported by Shannon[29]), the limiting t values for the stable perovskites being approximately 0.82–0.96.[30] For the stability of the perovskites, the octahedral factor ($r_B/r_O$) is as important as the tolerance factor. For $BiVO_3$ this value was found to be 0.457, which fits again within the stability range that is between 0.414–0.732.[31]. Although these numbers predict a stable $BiVO_3$ perovskite structure, no successful synthesis of $BiVO_3$ has yet been reported. Only one unsuccessful attempt has been published so far. In the 1970`s N. Ramadass et al.[32] fired a stoichiometric mixture of $Bi_2O_3$ and $V_2O_3$ in sealed evacuated silica tube. The product was not the $BiVO_3$ perovskite but described as having a cubic defect pyrochlore structure with a composition of $Bi_2V_2O_{7-y}$. Unfortunately, the report on the structural analysis of this pyrochlore is very deficient and does not allow us to judge on the correctness of the conclusions.

Because of the high technological interest of this material, we used theoretical and experimental approaches to answer the question whether the $BiVO_3$ perovskite is thermodynamically unstable or it just has not been synthesized yet due to experimental difficulties. To understand this we have undertaken investigation of the structural and dynamic stability of $BiVO_3$ perovskite by the

computational modeling. After the stability has theoretically been confirmed we turned our attention on the synthesis. We have performed an extensive experimental work to understand the chemical processes and interactions that cause difficulties with the synthesis of the $BiVO_3$. We present these processes in order to enable the synthetic chemists to build on this knowledge and eventually preform a successfully synthesis of this compound.

## II. Experimental

The computational model that we have used in the present quantum mechanical calculations is based on periodic boundary conditions at the Density Functional Theory (DFT) level of approximations using the ab-intio quantum mechanical package CRYSTAL09 (CR09).[33,34] In CR09, the Gaussian-type functions (GTF) localized at atoms are used as the basis set for an expansion of the crystalline orbitals. All electron basis set has been used for the lighter oxygen and vanadium atoms (O: 8-411(1d); V: 8-6-411(31d)),[35] while Hay and Wadt large-core (HAYWLC) pseudo-potentials were applied for the heavier bismuth atom.[36] Spin polarized unrestricted DFT calculations are performed using the B1WC functional. Exchange and correlation have been treated in the B1WC functional using the exchange functional Becke and the correlation functional WC with a 16% Fock exchange. Coulomb and exchange series evaluation was performed by a set of "cutoff" tolerances (ITOL*n*, *n*=1 to 5); see references[33,34] for more details. In the present study we have used high values for the ITOL*n* values (8, 8, 8, 8, 14) which reduces the numerical inaccuracies to a minimum. Reciprocal sampling has been performed by sampling the first Brillouin zone at a regular array (Pack-Monkhorst grid) of 6× 6 ×6 k-points (80 k-points in the irreducible part of the Brillouin zone) and a much denser grid of 312 k-points (10×10×10) for the evaluation of one electron properties. Convergence in the total energy has been set to $10^{-10}$ Hartrees. Atomic positions and the cell coordinates predicted by the SpuDS[37] were used as a

starting point and a complete geometry optimization has been performed by minimizing the forces using the BFGS algorithm as available in CR09. Vibrational frequencies at the Γ-point are calculated within the harmonic approximation. The dynamical matrix was computed by numerical evaluation of the first derivatives of the analytical atomic gradients. For a detailed description of the method and its recent applications we refer to a series of papers.[38.39]

Solid-state reactions between $Bi_2O_3$ and $V_2O_3$ were conducted in $N_2$ at atmospheric pressure (AP), and at low pressures (LP) of $10^{-6}$ bar. The starting reagents, $Bi_2O_3$ (Alfa Aesar, 99.975%) and $V_2O_3$ (Alfa Aesar, 97%) in 1:1 ratio were homogenized dry, in an agate mortar. For the AP experiments, the mixture was pressed into pellets (for a better contact between the precursors) and then heat treated at temperatures ranging from 400 to 900°C in a sealed tube furnace under $N_2$ (99.999%) atmosphere. In the case of LP experiments, the powders were inserted into quartz ampoules and vacuum sealed at a pressure of ~$10^{-6}$ bar. Reference samples consisting of $Bi_2O_3$ and $V_2O_3$ respectively, were heat treated separately at the same conditions as the stoichiometric mixtures. The phase characterization was carried out by x-ray powder diffraction using a PANalytical X-ray diffractometer with Cu $K_\alpha$ radiation ($\lambda$ = 0.154 nm), a step size of 0.017° and collection time of 25.8s per step. The diffraction patterns were recorded in the range $2\theta$ = 15-80°. The quantitative analysis of the phases was done using the PANalytical X'Pert HighScore Plus software.

## III. Results and discussion

### (1) Computational studies of structure stability

Since we lack geometric information to pursue the DFT simulations, we have used the SPUDS,[37] a crystallographic structure prediction and diagnostic software, for the generation of the lattice

parameters and atomic coordinates. The program calculates the optimal configuration of a given perovskite composition in ten Glazer tilt systems by distorting the structure in order to minimize the global instability index (GII) while maintaining the rigid octahedra. The structure with the minimum GII is considered to be stable, however, SPUD is only a semi-empirical software that needs verification of the results. The optimum magnitude of the octahedron tilting is calculated using the bond valence model as suggested by Brown[40] and is related to the minimum difference between the calculated bond valence and the formal charge. For a detailed description of the method we refer to Lufaso et al.[37]

Our analysis showed that $R\,\bar{3}c$ and Pnma are the two $BiVO_3$ structures with the minimum GII of 0.0048 and 0.00879, respectively. Perovskite systems with the tolerance factor in the range of 0.8-0.9 mostly adopt an orthorhombic structure [41] at low temperature, which indicates on Pnma to be more probable choice than the rhombohedral $R\,\bar{3}c$ . In addition, we performed a series of self-consistent field calculations on $R\,\bar{3}c$ and found difficulties in converging the calculations, which is reliable evidence that the $R\,\bar{3}c$ structure was wrongly predicted by SPUDS. We continued our studies on the next GII minimum, based on the orthorhombic Pnma structure, for which the convergence of the calculations was not a problem. The Pnma structure can be thought of as being formed by repeated tilting of the $VO_6$ octahedral units in a zig-zag manner ($GdFeO_3$ type distortion[42]) as shown in Fig. 1. The tilting can be assigned as two anti-phase tilts of equal magnitude with respect to the [100] and [001] pseudo cubic axes and an in-phase tilt with respect to the [010] pseudo-cubic axis (i.e., $a^-b^+a^-$).

The tilting results in a decrease in symmetry as well as in an increase in the size of the unit cell from one to four formula units. The total energy of the aristotype cubic and the hettotype orthorhombic structures after relaxing the geometry are presented in Table I.

As seen from the table, the ferromagnetic orthorhombic structure is 1.275 eV/f.u lower in energy compared to the cubic structure. Thus, structurally the orthorhombic phase is far more stable than the cubic. In addition, the B1WC functional predicts the electronic nature of the cubic structure as conducting while that of the orthorhombic structure as semiconducting. This further corroborates that the cubic structure is less likely to be the ground state of $BiVO_3$ crystal. Similar instabilities for the cubic structures are noticed for the other perovskites from the same family. For example, Ravindran et al.[43] has shown on the instability of the cubic phase of $BiFeO_3$ because of its higher energy (1.1 eV/f.u) compared to the R3c phase.

The Pnma structure has a point group symmetry of $D_{2h}$ (space group number 62 in the standard setting), with four formula units per unit cell. Therefore, there are four transition metal atoms in the unit cell and this allows assigning different anti-ferromagnetic structures in addition to the ferromagnetic structure. In our case, we have assigned all the possible three anti-ferromagnetic orderings, namely A-type (A-AFM), G-type (G-AFM) and C-type (C-AFM). The total energies of all three relaxed anti-ferromagnetic structures are also reported in Table 1. As it can be seen from the table, the energy difference between the ferromagnetic and the anti-ferromagnetic structures is very small. These nearly degenerate energies indicate on a high level of competition among the FM and the AFM states. However, the FM state still remains as slightly more stable than any other magnetic structure. Thus, we argue that the Pnma structure of $BiVO_3$ with ferromagnetic spin ordering is stable at low temperature. Further, in order to check the dynamic stability of $BiVO_3$ at its ground state, we have performed a phonon calculation at the center of the Brillouin zone. We calculated all the 60 modes, as suggested by the group theoretical analysis, and observed that all the modes are active. Among them, 24 are IR active and the remaining 36 are Raman active. We did not observe any soft modes, which suggest that $BiVO_3$ is dynamically stable. Although the calculated Born charge at the Bi site is close to +5 (well above the formal charge of +3), no off-

center driven instabilities are present. This might be because the system stabilizes with a very high rotation of the octahedra.

**(2) Experimental analysis of phase interactions**

Although our theoretical work suggests on the stability of $BiVO_3$ in its ground state, the efforts of the researcher[23] and our own efforts to synthesize the $BiVO_3$ perovskite by the solid-state reaction from $Bi_2O_3$ and $V_2O_3$ have failed and yielded multiphase samples. In this part of the study we have searched for the reason why $BiVO_3$ has not been synthesized yet and what processing conditions the researchers should target for a successful synthesis.

Our results indicate that the phase composition of nominal $BiVO_3$ after heat treatment depends on the heat treatment conditions and involves phases such as metallic Bi, $V_2O_5$, $BiVO_4$, $Bi_4V_2O_{10.5}$ and $Bi_{1.62}V_8O_{16}$. The phases with vanadium in different oxidation states are formed, even if a special care has been taken to perform the synthesis in oxygen-free atmosphere. The same phases resulted when we prepared a bismuth(III) vanadium(III) precursor by a wet-chemical synthesis method and crystallize the product in inert ($N_2$) atmosphere at temperatures ranging from 400 to 900$^o$C. This shows that the observed phases are formed as a result of a thermodynamic equilibrium at applied conditions while their formation is not subjected to the selected method of the synthesis. It is evident that the synthesis of $BiVO_3$ cannot be accomplished by a direct reaction of oxides under conventional conditions, although the computational modeling suggests $BiVO_3$ to be dynamically stable. Deeper understanding of the processes that dominate the interaction of $Bi^{3+}$ and $V^{3+}$-based species is required to predict the conditions of the synthesis. Since no $Bi_2O_3$-$V_2O_3$ phase diagrams or any information regarding their interactions are available in the literature, our further research has been directed into the studies of these interactions in order to identify the processes that avert the formation of $BiVO_3$. Firstly, two reference samples, $Bi_2O_3$ and $V_2O_3$, were separately heat

treated in $N_2$ at atmospheric pressure and in quartz ampoules in vacuum ($10^{-6}$ bar). The XRD analysis after the thermal treatment showed in both cases the same results: partial amorphisation associated with partial oxidation of the $V_2O_3$ to $VO_2$ phase (see Fig. 2).

The partial oxidation of the $V_2O_3$ phase could be caused by the residual oxygen in the atmosphere and/or by the oxygen species adsorbed on the surface of the $V_2O_3$ oxide. In the case of $Bi_2O_3$ no phase changes has been noticed after the heat treatment. Further experiments were performed on the equimolar mixtures of $V_2O_3$ and $Bi_2O_3$ which were heat treated at different temperatures from 300°C to 900°C. The experiments were again performed in $N_2$ and vacuum; however, no significant influence of the atmosphere has been detected. At 300°C, no interaction between the two oxides was observed. The product consisted of some $VO_2$ in accordance to the reference experiment. At 400°C, the first interaction between both phases was observed. The new phases that have formed are $Bi^0$ and $BiVO_4$ (see Fig. 3).

At the same conditions of the thermal treatment, the reference $Bi_2O_3$ sample was not reduced to metal Bi, but in the presence of $V_2O_3$, metal Bi appeared as a reaction product. In addition, the reaction yielded $BiVO_4$ phase with vanadium in 5+ valence state. This indicates that the direct reaction between $Bi_2O_3$ and $V_2O_3$ does not occur. The reaction is sequential, initially induced by an electron transfer from $V^{3+}$ on $Bi^{3+}$, i.e. solid-state redox reaction that yields $Bi^0$ and $V^{5+}$.

$$2/3Bi_2O_3 + V_2O_3 \rightarrow 4/3Bi^0 + V_2O_5 \quad \text{(i)}$$

At these conditions, $V_2O_5$ reacts further with unreduced $Bi_2O_3$ to form the $BiVO_4$ phase.

$$V_2O_5 + Bi_2O_3 \rightarrow 2BiVO_4 \quad \text{(ii)}$$

$Bi_2O_3$ oxidizes $V_2O_3$, but competitively also reacts with newly formed $V_2O_5$. As a consequence, the redox reaction stops before all V-oxides are consumed. Unfortunately, low electron density and consequent low x-ray scattering factors for V-oxides compared to Bi compounds make the XRD analysis of small concentrations of the V-oxides difficult. So, in these cases we have not been able to reliably detect and identify the remaining V-oxide phases. At temperatures above 500°C, other bismuth vanadates appear (see Fig. 4): predominantly $Bi_{1.62}V_8O_{16}$ and polymorphs of $Bi_4V_2O_{10.5}$, where V is again in the oxidation state lower than 5+.

As we know that the direct reaction between $Bi_2O_3$, $VO_2$ and $V_2O_3$ is not possible, the only reaction path that can result in the binary Bi-vanadates with $V^{3+}$ or $V^{4+}$, must go through the reduction of $V^{5+}$ in $BiVO_4$ at elevated temperature and low oxygen partial pressures.

$$5.62\ BiVO_4 + 4.38\ VO_x \xrightarrow{T > 600^oC} Bi_4V_2O_{10.5} + Bi_{1.62}V_8O_{16} \qquad \text{(iii)}$$

The coefficients in the eq. 3 are approximate as the V-oxides were not identified. The experiments show that the reduction-oxidation reaction occurs between $Bi^{3+}$ and $V^{3+}$ already at very low temperature between 300°C and 400°C. This solid-state redox reaction is a consequence of the tendency to form covalent bonding between the $Bi^{3+}$, $V^{3+}$ cations with O, because, in order to stabilize the $BiVO_3$ structure, a strong orbital interaction between $Bi^{3+}$ and $VO_6$ octahedra is, however, necessary (Bi-O distance of ~2.2 Å calculated by the ab-initio modeling). But in the present case, we observed that the activation energy for oxidizing the $V^{3+}$ is much lower compared to the stabilization energy of the $Bi^{3+}$ state. This facilitates a charge transfer between $V^{3+}$ and $Bi^{3+}$ at fairly low temperatures. The situation is different in the hollandite-type $Bi_{1.62}V_8O_{16}$ phase (where

Bi is in 3+ and V in 3+ and 4+ oxidation states) wherein the electron transfer between $Bi^{3+}$ and $V^{3+}$ does not take place even at high temperatures (of 800°C). This indicates higher activation energy for the reduction of $Bi^{3+}$ to the metallic state, probably because in the hollandite-type structure the Bi cations occupy much larger channels (here the Bi-O distance is ~2.5 Å) and therefore they interact only weakly and without covalent bonding with the $VO_6$ octahedra.

The theoretical and experimental studies of the $BiVO_3$ perovskite showed apparently contradictory results. While the computation modeling suggests the stability of $BiVO_3$ in its ground state, the stability could not be confirmed by a successful synthesis. The study of the chemical processes during the reaction between the nominal oxides revealed a competitive electronic process that at elevated temperatures prevails. With the combined theoretical and experimental study we showed that the formation of $BiVO_3$ requires a strong orbital coupling between $Bi^{3+}$ and $V^{3+}$. At such electronic state and at the selected processing temperatures, the activation energy for the electron transfer from V to Bi is exceeded. The solid-state redox reaction occurs and instead of $BiVO_3$, metallic Bi and oxidized V phases are formed. However, this result does not necessarily disprove the stability of $BiVO_3$ or the possibility of its formation at lower temperatures, for which the activation energy for the redox reaction is not exceeded. Consequently, low temperature synthesis methods, such as hydro(solvo)thermal or even ammonothermal, would be more likely to yield $BiVO_3$.

## IV. Conclusions

The results of our computational study show that $BiVO_3$ could adopt an orthorhombic (Pnma) structure which was found to be with 1.275 eV/f.u. more stable than the cubic one. Even if there is a high level of competition among the ferromagnetic and the antiferromagnetic states, we found

that the ferromagnetic state still remains as slightly more stable than any another magnetic structure at low temperature. We also analyzed the dynamic stability of $BiVO_3$ at its ground state through a zone centre phonon calculation. No soft modes showing off-centre driven instabilities are observed in the IR spectra, most probably, due to the structure stabilization by a higher degree of octahedra rotation rather than off-centering the Bi-cation. This enables us to conclude that the material is dynamically stable at low temperature and can be synthesized if right processing conditions are applied. Our experimental work, directed in the search for the right processing conditions, revealed the reduction-oxidation reaction between $Bi^{3+}$ and $V^{3+}$ as the process that averts the formation of $BiVO_3$. The strong orbital interaction of the $Bi^{3+}$ and $V^{3+}$ atoms with oxygen in $BiVO_3$ facilitates the electron transfer from V to Bi and destabilization of the structure. The interaction yield metallic Bi and $V_2O_5$ instead of $BiVO_3$. Despite the fact that this process prevents the formation of $BiVO_3$ at elevated temperatures it does not necessarily mean that $BiVO_3$ is not stable and cannot be synthesized at some more appropriate conditions. We suggest that successful synthesis of $BiVO_3$ might be accomplished by low-temperature synthesis methods were the activation energy for the reduction-oxidation process would not be exceeded.



**Acknowledgements**

The work has been supported by the Slovenian Research Agency research program P2-0337. The authors would like to thank HPC-EUROPA2 for providing access to the supercomputing facilities at the Barcelona Supercomputing Centre, Arctur d.o.o. for free access to their HPC facilities and to Prof. Dr. Gašper Tavčar and to Ph.D. student Aleš Štefančič from the Jožef Stefan Institute (Slovenia) for the support at the experimental work.

## References


1. G. G. Briand and N. Burford, 'Bismuth compounds and preparations with biological or medicinal relevance,' *Chem. Rev.*, 99 [9] 2601-57 (1999).
2. T. Takahashi and H. Iwahara, 'Oxide ion conductors based on bismuth sesquioxide,' *Mater. Res. Bull.*, 13 [12] 1447-53 (1978).
3. I. Zeljkovic, E. J. Main, T. L. Williams, M. C. Boyer, K. Chatterjee, W. D. Wise, Y. Yin, M. Zech, A. Pivonka, T. Kondo, T. Takeuchi, H. Ikuta, J. Wen, Z. Xu, G. D. Gu, E. W. Hudson, and J. Hoffman, 'Scanning tunnelling microscopy imaging of symmetry-breaking structural distortion in the bismuth-based cuprate superconductors,' *Nat. Mater.*, 11 [7] 585-89 (2012).
4. L. F. Mattheiss, E. M. Gyorgy, and D. W. Johnson Jr., 'Superconductivity above 20 K in the Ba-K-Bi-0 system', *Phys. Rev. B.,* 37 [7] 3745-46 (1988).
5. M. Mehring, 'From molecules to bismuth oxide/based materials: Potential homo- and heterometalic precursors and model compounds', *Coord. Chem. Rev.*, 251 [7-8] 974-1006 (2007).
6. P. Baettig, C. F. Schelle, R. Le Sar, U. V. Waghmare, and N. A. Spaldin, 'Theoretical Prediction of New High-Performance Lead-Free Piezoelectrics', *Chem. Mater.*, 17 [6] 1376-80 (2005).
7. J.Zylberberg, A. A. Belik, E. Takayama-Muromachiand, and Z. Ye, 'Bismuth Aluminate: A New High-$T_C$ Lead-Free Piezo-/Ferroelectric,' *Chem. Mater.,* 19 [26] 6385-90 (2007).
8. T. Zou, X. Wang, H. Wang, C. Zhong, L. Li, and I-Wei Chen, 'Bulk dense fine-grain $1-xBiScO_3–xPbTiO_3$ ceramics with high piezoelectric coefficient,' *Appl. Phys. Lett.,* 93 [19] 192913 3pp (2008).

9. K. Oka, M. Azuma, W.T. Chen, A.A. Belik, E. Takayama-Muromachi, M. Mizumaki, N. Ishimatsu, N. Hiraoka, M. Tsujimo, M.G. Tucker, J. P. Attfield, and Y. Shimakawa, 'Pressure-induced spin-state transition in $BiCoO_3$,' *J. Am. Chem Soc.,* 134 [27] 9438-43 (2010).

10. K. Ujimoto, T. Yoshimura, A. Ashida, and N. Fujimura, 'Direct piezoelectric properties of (100) and (111) $BiFeO_3$ epitaxial thin films,' *Appl. Phys.Lett*., 100 [10] 102901 3pp (2012).

11. Y. Zhang, A. M. Schultz, P. A. Salvador and G. S. Rohrer, Y. Zhang, A. M. Schultz, P. A. Salvador, and G. S. Rohrer, 'Spatially selective visible light photocatalytic activity of $TiO_2$/$BiFeO_3$ heterostructures,' *J. Mater. Chem*., 21 [12] 4168-74 (2011).

12. S. Li, Y.-H. Lin, B.-P. Zhang, Y. Wang, and C.-W. Nan, 'Controlled Fabrication of $BiFeO_3$ Uniform Microcrystals and Their Magnetic and Photocatalytic Behaviors;' *J. Phys. Chem. C* 114 [7] 2903-08 (2010).

13. R. Guo, L. Fang, W. Dong, F. Zheng, and M. Shen, 'Enhanced Photocatalytic Activity and Ferromagnetism in Gd Doped $BiFeO_3$Nanoparticles,' *J. Phys. Chem. C* 114 [49] 21390-96 (2010).

14. J. Wang, J. B. Neaton, H. Zheng, V. Nagarajan, S. B. Ogale, B. Liu, D. Viehland, V. Vaithyanathan, D. G. Schlom, U. V. Waghmare, N. A. Spaldin, K. M. Rabe, M. Wuttig, and R. Ramesh, 'Epitaxial $BiFeO_3$Multiferroic Thin Film Heterostructures,' *Science,* 299 [5613] 1719-22 (2003).

15. G. Catalan and J.F. Scott, 'Physics and applications of bismuth ferrite,' *Adv. Mater*., 21 [24] 2463-85 (2009).

16. Z. H. Chi, C. J. Xiao, S. M. Feng, F. Y. Li, C. Q. Jin, X. H. Wang, R. Z. Chen, and L. T. Li, 'Manifestation of ferroelectromagnetism in $BiMnO_3$,' *J. Appl. Phys.,* 98 [10] 103519 5pp (2005).

17. N. A. Hill and K. R. Rabe, 'First-principles investigation of ferromagnetism and ferroelectricity in bismuth manganite,' *Phys. Rev. B* 59 [13] 8759–69 (1999).

18. R. Ramesh and N. A. Spaldin, 'Multiferroics: progress and prospects in thin films,' *Nat. Mater.*, 6 [1] 21-29 (2007).

19. A. A. Belik, S.Iikubo, K. Kodama, N. Igawa, S. Shamoto, S. Niitaka, M. Azuma, Y. Shimakawa, M. Takano, F. Izumi, and E. Takayama-Muromachi, 'Neutron Powder Diffraction Study on the Crystal and Magnetic Structures of $BiCoO_3$,' *Chem. Mater.,* 18 [3] 798–803 (*2*006).

20. N. A. Hill, 'First Principles Search for Multiferroism in $BiCrO_3$,' *J. Phys. Chem. B*, 106 [13] 3383–88 (2002).

21. M. Azuma, W. Chen, H. Seki, M. Czapski, S. Olga, K. Oka, M. Mizumaki, T. Watanuki, N. Ishimatsu, N. Kawamura, S. Ishiwata, M. G. Tucker, Y.Shimakawa, and J. P.Attfield, 'Colossal negative thermal expansion in $BiNiO_3$ induced by intermetallic charge transfer,' *Nat. Commun*., 2 [347] 1–5 (2011).

22. M. Q. Cai, X. Tan, G. W. Yang, L. Q. Wen, L. L. Wang, W. Y. Hu, and Y. G. Wang, 'Giant Magneto-Optical Kerr Effects in Ferromagnetic Perovskite $BiNiO_3$ with Half-Metallic State,' *J. Phys. Chem. C*, 112 [42] 16638–642 (2008).

23. A. A. Belik, 'Polar and non polar phases of $BiMO_3$: A review,' *J. Solid State Chem*., (2012) doi:10.1016/j.jssc.2012.01.025. (in press)

24. A. A. Belik, T. Wuernisha, T. Kamiyama, K. Mori, M. Maie, T. Nagai, Y. Matsui, and E. Takayama-Muromachi, 'High-Pressure Synthesis, Crystal Structures, and Properties of Perovskite-like $BiAlO_3$ and Pyroxene-like $BiGaO_3$,' *Chem. Mater.*, 18 [1] 133–39 (2006).

25. D. J. Payne, M. Robinson, R. G. Egdell, A. Walsh, J. McNulty, K.E. Smith, and L. F. J. Piper, 'Nature of the Bismuth Lone-Pair in $BiVO_4$,' *Appl. Phys. Lett.*, 98 [21] 212110 3pp (2011).

26. S. Murugesan, M. N. Huda, Y. Yan, M. M. Al-Jassim, and V. Subramanian, 'Band-Engineered Bismuth Titanate Pyrochlores for Visible Light Photocatalysis,' *J. Phys. Chem. C*, 114 [23] 10598–605 (2010).

27. A. Kudo, K. Omori, and H. Kato, 'A Novel Aqueous Process for Preparation of Crystal Form-Controlled and Highly Crystalline $BiVO_4$ Powder from Layered Vanadates at Room Temperature and Its Photocatalytic and Photophysical Properties,' *J. Am. Chem. Soc.*, 121 [49] 11459–467 (1999).

28. V. M. Goldschmidt, 'Die Gesetze der Krystallochemie' ('The laws of Cristallochemistry'), *Die Naturwissenschaften,* 14 [21] 477–85 (1928).

29. R. D. Shannon, 'Revised Effective Ionic Radii and Systematic Studies of Interatomic Distances in Halides and Chaleogenides,' *Acta Crystallogr., Sect. A: Cryst. Phys., Diffr., Theor. Gen. Crystallogr.*, 32 [5] 751–67 (1976).

30. L. M. Feng, L. Q. Jiang, M. Zhu, H. B. Liu, X. Zhou, and C. H. Li, 'Formability of $ABO_3$ cubic perovskites,' *J. Phys. Chem. Solids*, 69 [4] 967–74 (2008).

31. Z. L. Wang and Z. C. Kang, 'Perovskites and Related Systems'; pp. 93–149 in '*Functional and Smart Materials: Structural Evolution and Structure Analysis.* Kang Plenum Publishing, New York, 1998.

32. N. Ramadass, T. Palanisamy, J. Gopalakrishnan, G. Aravamudan, and M. V. C. Sastri, 'Some $ABO_3$ oxides with defect pyrochlore structure,' *Solid State Commun. Solid State Commun*., 17 [4] 545–47 (1975).

33. R. Dovesi, V. R. Saunders, C. Roetti, R. Orlando, C. M. Zicovich-Wilson, F. Pascale, B. Civalleri, K. Doll, N. M. Harrison, I. J. Bush, Ph. D'Arco, and M. Llunell, in *CRYSTAL09 User's Manual.* University of Torino, Torino, 2010.

34. R. Dovesi, R. Orlando, B. Civalleri, R. Roetti, V. R. Saunders, and C. M. Zicovich-Wilson, 'CRYSTAL: a computational tool for the ab initio study of the electronic properties of crystals,' *Z. Kristallogr*, 220 [5-6] 571–73 (2004).

35. Available at: www.crystal.unito.it/basis_sets/ptable.html.

36. M. Goffinet, P. Hermet, D. Bilc, and P. Ghosez, 'Hybrid functional study of prototypical multiferroic bismuth ferrite,' *Phys. Rev. B,* 79 [1] 014403 9pp (2009).

37. M. W. Lufaso and P.M. Woodward, 'Prediction of the crystal structures of perovskites using the software program SPuDS,*' Acta Crystallogr., Sect. B: Struct. Sci.* 57 [6] 725–38 (2001).

38. C. M. Zicovich-Wilson, F. Pascale, C. Roetti, V. R. Saunders, R. Orlando, R. Dovesi, 'Calculation of the vibrational frequencies of a alpha-quartz,' *Comput. Chem.*, 25 [15] 1873–81 (2004).

39. L. Valenzano, Y. Noel, R. Orlando, C. M. Zicovich-Wilson, M. Ferrero, and R. Dovesi, 'Ab initio vibrational spectra and dielectric properties of carbonates: magnesite, calcite and dolomite,' *Teor. Chem. Acc.,* 117 [5-6] 991-1000 (2007).

40. I. D. Brown, 'The Bond Valence Model'; pp 26–39 in *The chemical bond in inorganic chemistry: the bond valence model.* Oxford University Press, New York, 2006.

41. H. L. Yakel Jr., 'On the Structure of some Compounds of Perovskite Type,' *Acta Crystallogr*. 8 [7] 394-98 (1955).

42. L. Vasylechko L., A. Matkovskii, D. Savytskii, A. Suchocki, and F. Wallrafen, 'Crystal structure of GdFeO-type rare earth gallates and aluminates,' *J. Alloys Compd.* 291 [1-2] 57-65 (1999).

43. P. Ravindran, R. Vidya, A. Kjekshus, H. Fjellaåg, and O. Eriksson, 'Theoretical investigation of magnetoelectric behavior in $BiFeO_3$,' *Phys. Rev. B*, 74 [22] 224412 18pp (2006).

## Figure captions

**Fig. 1.** Pnma structure (left) is shown as a distorted derivative of the cubic structure (right). For a clear indication of the nature of the distortion, the undistorted cubic part is notated as a blue square. Coloring of the atoms is as follows: Bi (dark magenta), V (dark orange), O (dark brown).

**Fig. 2.** X-ray diffraction patterns of $V_2O_3$ before and after thermal treatment at 400$^{o}$C.

**Fig. 3.** X-ray diffraction patterns of the $Bi_2O_3$:$V_2O_3$ (1:1) samples before (raw) and after the thermal treatment at 300 and 400$^{o}$C (magnification of the region where the reflections of the new phases appear.

**Fig. 4.** X-ray diffraction patterns of the $Bi_2O_3$:$V_2O_3$ (1:1) samples heated at 800 and 900$^{o}$C respectively.

## Tables

**Table I.** Total energy per formula unit (f.u) of the cubic $(Pm\bar{3}m)$ and the orthorhombic $(Pnma)$ $BiVO_3$. The energy of the ferromagnetic *Pnma* structure is taken as the reference energy. The total energy corresponding to different antiferromagnetic settings of *Pnma* (A-AFM, C-AFM, and G-AFM) is also provided

| Structure | $Pm\bar{3}m$ $FM$ | $Pnma$ $(FM)$ | $Pnma$ $(A-AFM)$ | $Pnma$ $(G-AFM)$ | $Pnma$ $(C-AFM)$ |
|---|---|---|---|---|---|
| Total Energy (eV/f.u.) | -31955.67891 | -31956.95370 | -31956.92895 | -31956.90702 | -31956.92593 |
| $\Delta E = (E - E^{FM}_{Pnma})$(eV) | 1.275 | 0.0 | 0.02475 | 0.0466 | 0.027 |

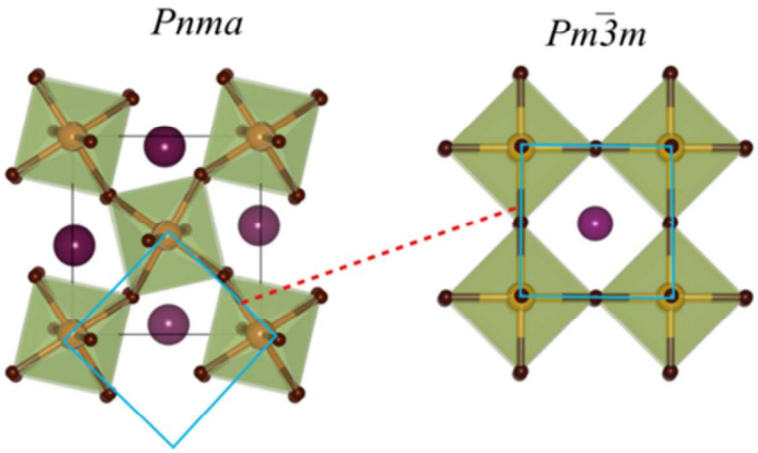


Fig. 1. Pnma structure (left) is shown as a distorted derivative of the cubic structure (right). For a clear indication of the nature of the distortion, the undistorted cubic part is notated as a blue square. Coloring of the atoms is as follows: Bi (dark magenta), V (dark orange), O (dark brown).

595x342mm (90 x 90 DPI)

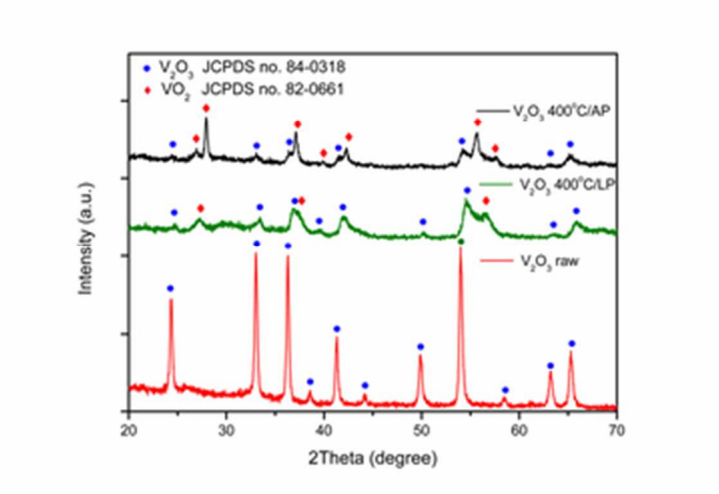


Fig. 2. X-ray diffraction patterns of V2O3 before and after thermal treatment at 400oC.
15x10mm (600 x 600 DPI)

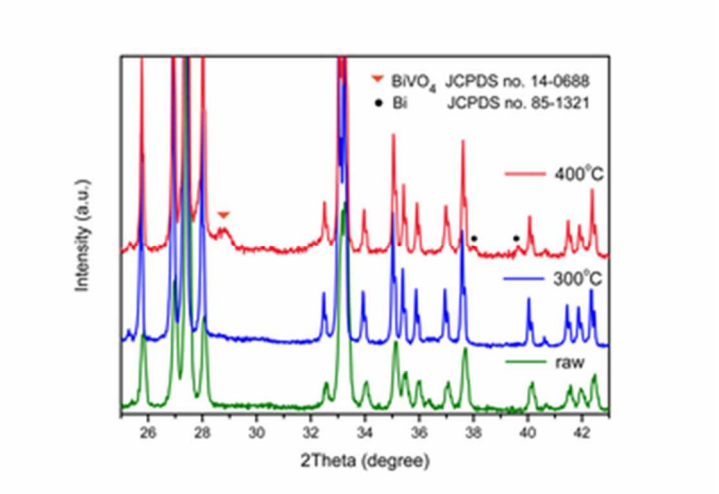


Fig. 3. X-ray diffraction patterns of the Bi2O3:V2O3 (1:1) samples before (raw) and after the thermal treatment at 300 and 400oC (magnification of the region where the reflections of the new phases appear. 15x10mm (600 x 600 DPI)

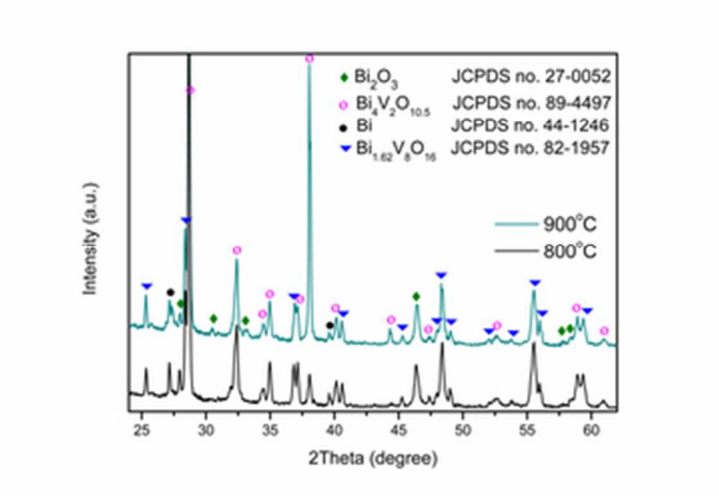


Fig. 4. X-ray diffraction patterns of the Bi2O3:V2O3 (1:1) samples heated at 800 and 900oC respectively. 15x10mm (600 x 600 DPI)